Werk

Jahr: 1985
Kollektion: fid.geo
Signatur: 8 Z NAT 2148:56
Digitalisiert: Niedersächsische Staats- und Universitätsbibliothek Göttingen
Werk Id: PPN1015067948_0056
PURL: http://resolver.sub.uni-goettingen.de/purl?PPN1015067948_0056

LOG Id: LOG_0034
LOG Titel: Source orientation from grid test and synthetic seismograms and an application to the Ibbenbüren earthquake of July 1981
LOG Typ: article

Übergeordnetes Werk

Werk Id: PPN1015067948
PURL: http://resolver.sub.uni-goettingen.de/purl?PPN1015067948
OPAC: http://opac.sub.uni-goettingen.de/DB=1/PPN?PPN=1015067948

Contact

Niedersächsische Staats- und Universitätsbibliothek Göttingen
Georg-August-Universität Göttingen
Platz der Göttinger Sieben 1
37073 Göttingen
Germany
Email: gdz@sub.uni-goettingen.de

J Geophys (1985) 56:147–152

Journal of Geophysics

Source orientation from grid test and synthetic seismograms and an application to the Ibbenbüren earthquake of July 1981

K.-G. Hinzen* and H. Krummel
Institut für Geophysik, Ruhr-Universität Bochum, Universitätsstraße 150, D-4630 Bochum, Federal Republic of Germany

Abstract. A fault-plane solution technique for regional seismic events is developed. A flexible grid test procedure is used to make combined use of *P*-wave first-motion readings and angles of polarisation of *S* waves. All solutions, which are compatible with the measurements on the basis of a double-couple source are found in this way. Synthetic seismograms calculated with the reflectivity method are used to obtain the most reliable among these solutions.

The procedure is tested with data from the 13 July 1981 Ibbenbüren event ($M_L = 4.1$). Seventeen *P*-wave first-motion readings and one angle of polarisation leave 102 out of 93,312 solutions which are compatible with the double-couple model when a 5° increment of strike-, dip- and slip-angle is used. The synthetic seismograms show that a mechanism of strike-slip type is a reasonable model. This result is in contrast to a normal-fault mechanism from a former graphical fault-plane solution.

Key words: Fault-plane solution – Angle of polarisation – Grid test – Synthetic seismograms

Introduction

Fault-plane solutions are a common and basic tool in the determination of seismic source orientations. For local and regional events the focal sphere is often poorly covered with stations reporting clear *P*-wave first-motion readings (Engdahl and Kisslinger, 1977). In order to compensate for this lack of information parameters other than *P*-wave first motions have been introduced to fault-plane solution programs. Shapira and Båth (1978) use the amplitudes of *P* waves; Kisslinger (1980) and Kisslinger et al. (1981) introduced the amplitude ratio of *SV* and *P* waves recorded on the vertical component of near stations. Most of these methods use only one parameter derived from the seismogram. In many cases the quality of data is heterogeneous. Determination of *P*-wave first motions may be possible from analog seismograms; while amplitudes, amplitude ratios or angles of polarisation of *S* waves are more easily measured with three-component digital recording stations. Therefore, it is desirable to use a combination of parameters from seismograms of different quality in one calculation. This desire supposes a flexible algorithm for the numerical application.

In least-squares algorithms, which are often used in fault-plane solution techniques (Kisslinger et al., 1981; Stevens, 1964; Udias, 1964), it is difficult to combine different parameters, especially when *P*-wave first motions are concerned (Dillinger et al., 1972). Due to the nonlinearity of the problem, a bad choice of starting solution for the least-squares fit may lead to an incorrect orientation.

The implementation of a systematic trial-and-error method, or so-called 'grid method', can avoid these difficulties. Langston (1982) uses a grid method to model teleseismic records of *P* and *SH* waveforms to get the orientation of the source. Pearce (1977; 1979a, b; 1981) searches, in a systematic way, for orientations which are compatible with the amplitude ratios of *P*, *pP* and *sP* waves from teleseismic events. In the following, a flexible procedure is described which uses different parameters in the search for possible source orientations. Special emphasis is given to the angle of polarisation of *S* waves. The procedure is applied to a regional earthquake of 07.13.1981 at Ibbenbüren, which has already been examined by a common graphic fault-plane solution technique (Harjes et al., 1983).

The results of the grid test are used for the calculation of synthetic seismograms with the reflectivity method (Fuchs, 1968; Fuchs and Müller, 1971; Kind, 1978; 1979) in order to show which of the possible orientations gives the best fit to the data.

Description of the grid method

The orientation of a pure double-couple source is completely described by three angles:

ϕ – strike of fault plane
δ – dip of fault plane
λ – slip angle.

These angles define the space of orientation in which the possible solutions have to be searched for. They are measured in the same sense as described by Aki and Richards (1980, Fig. 4.13). The angular boundaries for the search are influenced by symmetry properties of *P*- and *S*-wave radiation patterns. The radiation patterns for a double-couple source in terms of ϕ, δ, λ, as well as azimuth θ and take-off angle i of the ray are given, for example, by Aki and Richards (1980, p. 115).

If the symmetry properties caused by the interchange of fault and auxiliary plane, are neglected, the angular

* *Present address:* Bundesanstalt für Geowissenschaften und Rohstoffe, Stilleweg 2, D-3000 Hannover

Offprint requests to: K.-G. Hinzen

boundaries necessary to include all orientations are given by Pearce (1979a):

$$\begin{aligned} d &\leqq \phi \leqq 2\pi \\ d &\leqq \delta \leqq \pi \\ d &\leqq \lambda \leqq \pi, \end{aligned} \tag{1}$$

where d is the increment of the angles of orientation which controls the total number of possible orientations.

Figure 1 shows a schematic flow chart of the implemented procedure. The input parameters are the number of stations, azimuth and take-off angles for observations consisting of P-wave first motions or angles or polarisation of S waves. For every angle of polarisation a confidence interval is needed. This is calculated from the rectilinearity of the hodogram of the S phase (Hinzen, 1984). The greater the deviation from linear polarisation, the smaller is the number of rejected solutions. The program starts with the initialisation of a field containing all possible solutions. That means all orientations are possible at the start of the grid test. The number of possible solutions grows rapidly with decreasing increments d. Therefore, 15 solutions were encoded in one 16-bit integer word.

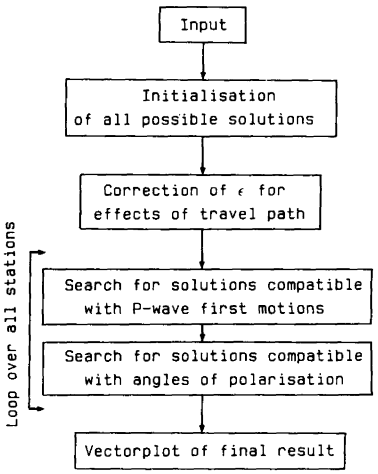

Fig. 1. Schematic flow chart of the grid test procedure for fault-plane solutions

The concept of focal sphere, introduced by Koning (1942) and Ritsema (1958), requires all data to be reduced to the values at the source. The data must be corrected for the influence of the travel path. The polarity of direct or refracted P waves does not change for regional or local distances in this reduction.

The influence of the free surface and reflection and transmission at boundaries on the angle of polarisation must be corrected. Båth (1961) solved the equations of motion for a plane wave incident on a plane boundary for several boundary conditions. In this way he could calculate the change of the angle or polarisation. The angle of polarisation, which is defined as

$$\varepsilon = \arctan \frac{A_{SH}}{A_{SV}} \tag{2}$$

is measured clockwise from the vertical in the interval

$$0 \leqq \varepsilon < \pi. \tag{3}$$

A_{SH} and A_{SV} are the amplitudes of SH and SV components, respectively.

The ratio of the angle of polarisation of the reflected wave and the incident wave is:

$$\frac{\tan \varepsilon_R}{\tan \varepsilon} = \frac{A^R_{SH}/A_{SH}}{A^R_{SV}/A_{AV}} \tag{4}$$

A^R_{SH}/A_{SH} is the reflection coefficient for the SH component; A^R_{SV}/A_{SV} the reflection coefficient for the SV component. In the case of refracted waves, the ratio of the angles of polarisation is:

$$\frac{\tan \varepsilon_T}{\tan \varepsilon} = \frac{A^T_{SH}/A_{SH}}{A^T_{SV}/A_{SV}} \frac{\beta_2}{\beta_1}. \tag{5}$$

A^T_{SH}/A_{SH} and A^T_{SV}/A_{SV} are the transmission coefficients and β_1 and β_2 denote the S-wave velocities in media 1 and 2, respectively. If the elastic parameters of the media are known, the changes of the angle of polarisation can be calculated.

After correction of the input data, the grid test procedure is made for every first-motion direction and angle of polarisation. The theoretical radiation value is compared with the measured value. If the first motion reading does not agree with the theoretical value or if the calculated angle of polarisation is not within the limits for the measured value, the orientation is rejected from the set of possible solutions. To avoid a strong influence of P readings close to nodal planes, which may be uncertain, solutions are kept as possible orientations if the theoretical radiation value for the P amplitude is smaller than a chosen fraction of the maximum amplitude. Normally a fraction of 5% is used. At the end of the test only those solutions, which are compatible with all measurements, remain.

The solutions are printed and displayed in a vectorplot (Pearce, 1977). In this plot, every combination of dip and slip angle is represented by a point in a grid. A possible solution is then indicated by a vector originating there and pointing in the direction of the fault-plane strike.

Application of the grid method

The grid method is applied to an earthquake ($M_L = 4.1$) which occurred on the 13 July 1981 near Ibbenbüren in the north-west part of the Teutoburger Wald (7°42.5′ E, 52°15.7′ N). The source orientation of this event has already been examined by the common graphical method in an earlier paper (Harjes et al., 1983), hereafter called Paper 1. In this solution, 19 P-wave first motions of European stations were used. The mechanism was interpreted as a normal fault on a N207° E-striking and either 60° NW- or 30° SE-dipping plane. Due to the lack of near stations, the position of the SE-dipping plane remained uncertain. The first-motion readings of two French stations disagreed with this solution.

In order to fit synthetic seismograms (see next section) to the recording of BUG, the crustal model of Paper 1 was modified. The wave velocities of the new model are given in Fig. 2. Take-off angles and corrections for ε were calculated on the basis of this model.

Input data for the grid test were the same first-motion readings as in Paper 1. If all 19 readings are used, none of the 93,312 solutions ($d = 5°$) remain possible, indicating that a pure double couple can not explain the observations. The two compressional readings at SSF and MZF have been omitted in a second test, as it was in the interpretation of Paper 1. In this case, 2152 solutions are compatible with

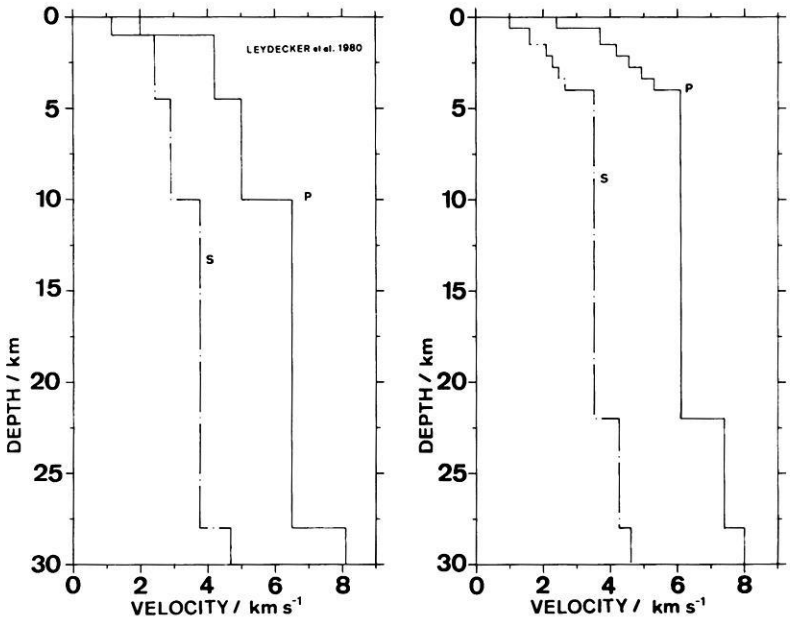

Fig. 2. Distribution of velocities of seismic waves. The *left model* (Leydecker et al., 1980) was used in Paper 1 (Harjes et al., 1983) and for the calculation of the synthetic seismogram in Fig. 7. The *right part* shows the modified model. This was used for the grid tests and synthetic seismograms of Fig. 8

the remaining observations. The solutions are displayed in the vectorplot of Fig. 3. The solution of Paper 1 is inducated in this figure by a small arrow and a capital 'A'. From this plot it becomes obvious that the solution of Paper 1 was subjectively selected by the interpreter from a great variety of possible solutions. In the vectorplot, most orientations with $\delta < 80°$ in the range of thrust mechanisms and normal-fault mechanisms with $125° \leqq \delta \leqq 150°$ are rejected.

In order to use more information from the digital three-component registration at BUG, the angle or polarisation of the *S* wave was determined. Figure 4 shows the hodogram of the ground movement with a duration of 1.6 s. By calculating the eigenvalues of the covariance matrix (Kanasewich, 1975) the angle of polarisation is found to be $\varepsilon_{BUG} = 136°$ with a rectilinearity of $R = 0.97$. ε_{BUG} was interpreted to belong to the S_g phase with a take-off angle $i = 36.5°$. The angle $\varepsilon_{BUG} = 136° \pm 15°$ leaves 14,928 compatible solutions, which are shown in the vectorplot of Fig. 5.

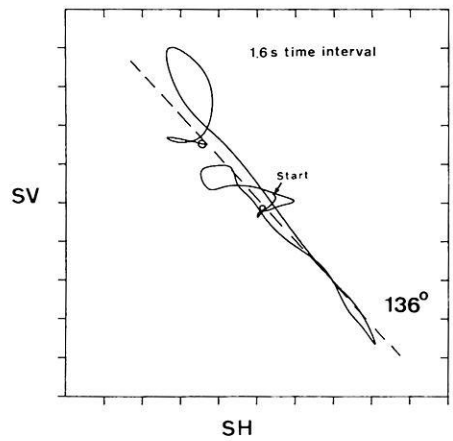

Fig. 4. Hodogram of the *S* wave of the 13 July, 1981, Ibbenbüren event derived from the seismogram of station BUG. The time interval is 1.6 s. The angle of polarisation is $\varepsilon = 136°$ with a rectilinearity of $R = 0.97$

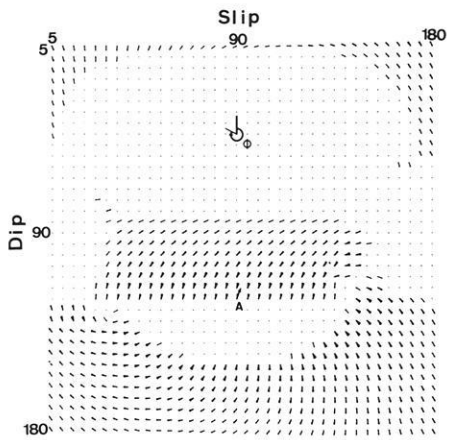

Fig. 3. Vectorplot of 2152 solutions which are compatible with 17 *P*-wave first-motion readings. The *small arrow* indicates the graphical solution of Paper 1 (see text for details). The *insert* shows the sense in which the strike of the fault planes, ϕ, is measured

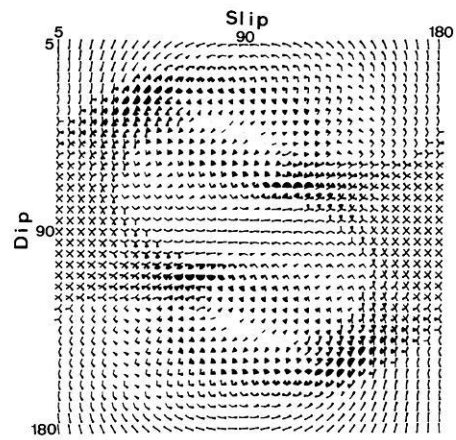

Fig. 5. Vectorplot of 14,928 solutions which are compatible with the angle of polarisation at BUG ($136° \pm 15°$)

A great variability of orientations becomes obvious. Fig. 6 shows the 102 solutions which agree with the first-motion readings and the angle of polarisation at BUG. The orientations form three ensembles in the vectorplot. The orientation from Paper 1 is indicated by a small arrow and a capital 'A'. Synthetic seismograms are calculated for the orientations B, C and D in the next section. A small deviation of take-off angle i does not change the results significantly. Even if the S phase is interpreted as S_n ($i=27°$), the solutions B, C and D remain possible. The theoretical values of ε are still within the interval of $\Delta\varepsilon = \pm 15°$ centred at the measured value. The inserts in Fig. 6 give the projections of the lower focal hemisphere of the labelled solutions. Areas of compressional P-wave first motions are black, as usual.

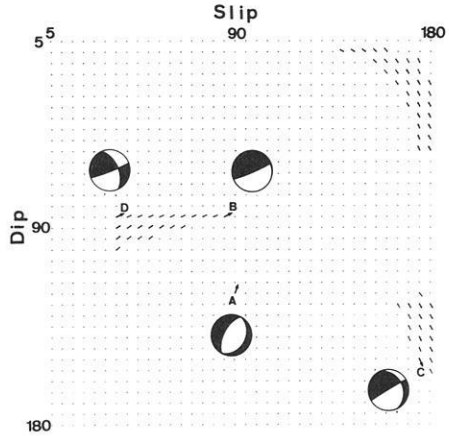

Fig. 6. Vectorplot of 102 solutions which are compatible with 17 P-wave first-motion readings and the angle of polarisation of the S wave recorded at BUG. Synthetic seismograms of those source orientations indicated by *small arrows* and *capital letters* are shown in Fig. 8. The *inserts* give the projections of the lower focal hemispheres for the labelled solutions. The *black quadrants* have compressional P-wave first motions

Synthetic seismograms

Synthetic seismograms of the 13 July, 1981, Ibbenbüren event have been calculated using the reflectivity method (Kind, 1978; 1979). The initial velocity model (Fig. 2) was that of Paper 1 after Leydecker et al. (1980). Additional information was provided by logs of the nearby Münsterland I well (Andres and Lichtenberg, 1963) and results of seismic refraction experiments (Mooney and Prodehl, 1978). The seismograms calculated with the velocity structure from Paper 1 showed reasonable agreement of theoretical and measured travel times of P and S waves at the station BUG. However, the surface wave trains observed at BUG could not be explained by this model. In Fig. 7, the bandpass-filtered (0.05–2.0 Hz) vertical component of the displacement seismogram from station BUG is compared with the synthetic seismogram calculated for the initial model. The filter was applied in order to get the same frequency content in measured and calculated seismograms. The reading of the polarity of P and the measurement of the angle or polarisation were made on the original seismograms with an upper frequency limit of 25 Hz (−3dB). The synthetic seismogram in Fig. 7 is dominated by body waves. The two surface wave groups of the observation are not visible.

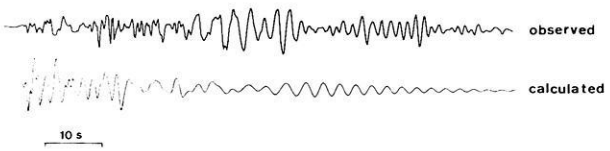

Fig. 7. The *upper trace* is the vertical component of the bandpass-filtered (0.05–2.0 Hz) displacement seismogram observed at BUG. The *lower trace* is a synthetic seismogram calculated with the source orientation from Paper 1 and the velocity structure after Leydecker et al. (1980). Misfits of amplitude ratios and within the surface waves are obvious

From information provided by the log, the P-wave velocities were reduced to a value of 2.4 km/s in the upper 600 m and five layers were introduced in the depth range from 0.6 km to 4.0 km to form a velocity gradient. The depth of the layer with P-wave velocity greater than 6 km/s was lowered to 22 km. By making these changes, the observed surface waves could be modelled.

In order to fit the time interval between the P phase and the surface wave arrivals, the velocity ratio α/β was increased from $\sqrt{3}$ to values between 2.4 and 2.0 in the first 4 km and was left at a value of $\sqrt{3}$ below this depth. The shape and duration of surface waves turned out to be very sensitive to these changes. Finally, by making the described changes to the velocity model (Fig. 2) the observed arrival times of P and S and the surface waves could be explained quite reasonably.

Source depth and source orientation were varied in order to fit amplitude ratios within the seismogram. The amplitudes of the surface waves are strongly influenced by the depth of the source. A set of seismograms was calculated with source depths in the range from 0.1 km to 10 km. Hypocentres shallower than 0.5 km and deeper than 5.0 km could be excluded by these calculations. The best fits were achieved with a source in the second layer between 0.6 km and 1.5 km. This agrees with the results of the macroseismic survey described in Paper 1, where a source depth of 2.0 ± 0.5 km was found.

The amplitude ratio of P and S waves is a good indicator for a correct orientation of the double-cpuple source. In the grid test procedure, 102 orientations agreed with the measured P-wave first motions of 17 stations and the angle of polarisation of S at BUG. About 20 orientations were chosen from the three ensembles in the vectorplot of Fig. 6 to calculate synthetic seismograms. Three examples are shown in Fig. 8. The upper and lower traces in this figure show the registration of station BUG (same as in Fig. 7) for comparison. P and S arrival times are given by arrows. The horizontal bar in the upper trace indicates the time interval of the hodogram in Fig. 4. The traces denoted B, C and D are calculated with the modified model and the orientations of the double couple given for each seismogram within the figure. These orientations are indicated in the vectorplot (Fig. 6) by small arrows and the corresponding focal spheres. The seismogram A is calculated with the model from this paper and the source orientation from Paper 1. The misfit of the amplitude ratio of P and S is obvious in cases A, B and C. The orientations A, B and C show amplitude ratios of P to S which are greater than or equal to one. The measured ratio from the

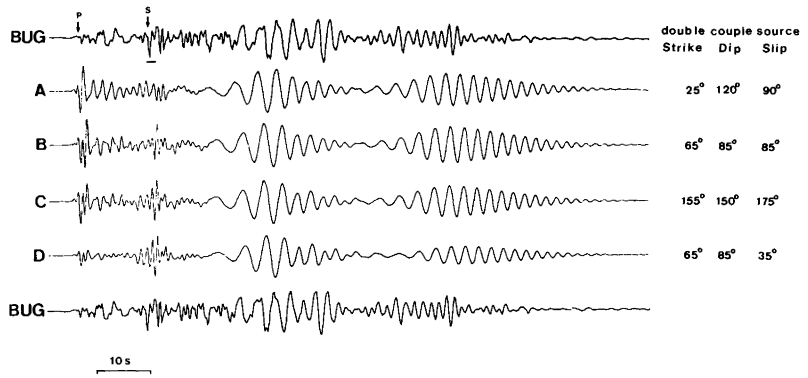

Fig. 8. Comparison of the seismogram recorded at BUG and synthetic seismograms for the 13 July, 1981, Ibbenbüren event. The orientation of the double-couple source for seismograms A, B, C and D is given next to each trace. A is the orientation derived in Paper 1 (see text for detail). The best fit is achieved with orientation D. The *bar* in the first trace shows the time interval of the hodogram in Fig. 4. The polarity of the traces A, B, C and D is reversed with respect to the measured seismogram

BUG seismogram is smaller than 0.5. Orientation D demonstrates the best fit within the possible solutions from the grid test. The projection of the nodal planes for solution D is shown in Fig. 9 (continuous lines). The dashed lines in the same figure give the position of nodal planes from the solution of Paper 1.

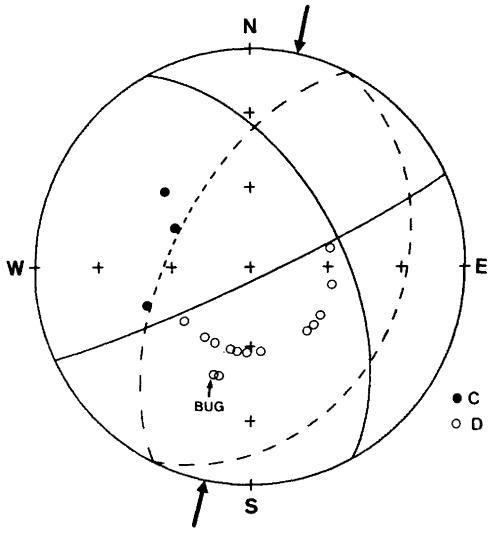

Fig. 9. Equal area projection of the lower focal hemisphere for the 13 July, 1981, Ibbenbüren event. Compressions and dilatations are shown by *closed and open circles*, respectively. The *dashed lines* are the nodal planes of the solution from Paper 1. The *continuous lines* give the orientation of the nodal planes of solution D from this paper. The *arrows* show the direction of the horizontal component of maximum compressive stress from this solution

Discussion and conclusions

The determination of fault-plane solutions for regional seismic events is problematic if only a few reliable *P*-wave first-motion readings are available. In such cases the solutions are often affected by the subjective influence of the interpreter.

A systematic search for solutions in the space of source orientations gives all orientations which agree with the data. The parameters derived from the seismograms may be polarities as well as amplitude ratios or angles of polarisation. In this paper, for example, polarities of *P*-wave first motions and angles of polarisation of *S* waves are used. The selected source orientations can be used for calculation of synthetic seismograms. In this way, the amount of calculation time is normally smaller than if the source orientation is searched for only by forward modelling with synthetic seismogram techniques in a trial-and-error sense.

An $M_L = 4.1$ event (13 July, 1981) at Ibbenbüren (FRG) is used to test the applicability of the procedure. Seventeen *P*-wave first motions and one angle of polarisation leave 102 solutions out of a possible 93,312 source orientations, if the increment of the angles of orientation is 5°. An earlier interpretation of the double-couple orientation on the basis of the classical graphic fault-plane solution technique resulted in a normal fault mechanism on a N207°E-striking and 60°NW- or 30°SE-dipping plane. This orientation is one of 2152 solutions which agree with the 17 *P*-wave first motions, but it disagrees with the angle of polarisation of *S* at BUG. A disagreement is also obvious between the measured seismogram and the calculated seismogram for the orientation from Paper 1. While the amplitude ratio of *P* to *S* is greater than one in the synthetic seismogram, it is smaller than 0.5 in the measured one. The amplitude ratio of *P* to *S* is strongly influenced by the orientation of the double-couple source. The best fit is achieved with solution D, which is a sinistral strike-slip motion on the ENE-WSW-striking plane or a dextral motion on the NNW-SSE-striking plane.

In Paper 1, an activation of the graben structure within the 'Ibbenbürener Bergplatte' was assumed to be the tectonic explanation for the earthquake. The main argument for this interpretation was the parallel trend of the assumed fault plane of solution A and the strike of the tectonic elements in the region. Solution D from this paper seems more trustworthy to the authors, due to the grid test and synthetic seismograms. This makes the former interpretation questionable. The direction of the horizontal component of maximum compressive stress is N13°E in solution D, indicated by two arrows in Fig. 9. This direction deviates significantly from the value of the mean direction for central Europe (N142°E $\pm$ 20°), which was derived by Ahorner (1975) from earthquake mechanisms and in situ stress measurements. In situ stress measurements during the last decade show directions approximately EW for boreholes within the Lower Saxonian Block (Rummel et al., 1983). Among these, a hydraulic fracturing experiment close to Bielefeld (Rummel and Baumgärtner, 1982) was the nearest to the 'Ibbenbürener Bergplatte'. The direction of the maximum horizontal stress was found to be N108°E. Therefore one would expect, from the fault-plane solution, a direction closer to the regional stress field direction for central Europe. Since it seems unlikely that the present local stress

field is still dominated by the tectonic evolution of the 'Ibbenbürener Bergplatte' and considering the shallow focal depth (1.5–2.0 km), a possible connection between mining activity in the area and earthquake occurrence can not be fully ignored. Mineworks within the 'Ibbenbürener Bergplatte' range down to a depth of more than 1 km. The influence of mineworks on the local stress field components could explain the deviating direction of maximum compressive stress.

Acknowledgements. The authors would like to thank H.-P. Harjes, F. Rummel and an anonymous reviewer for helpful comments. We are grateful to R. Kind for providing the reflectivity program. The grid tests were calculated on a HP 1000 computer of the Institute of Geophysics, while the synthetic seismograms were calculated with a CDC 175 of the 'Rechenzentrum der Ruhr-Universität'.

References

Ahorner, L.: Present day stress field and seismotectonic block movements along major fault zones in Central Europe. Tectonophys., **29**, 233–249, 1975

Aki, K., Richards, P.G.: Quantitative seismology. Vol. 1. San Francisco: W.H. Freeman, 1980

Andres, J., Lichtenberg, K.: Die Auswertung der seismischen Voruntersuchungen auf Grund der durch die Bohrung Münsterland I gewonnenen Daten. Fortschr. Geol. Rheinl. und Westfalen, **11**, Krefeld. 1963

Båth, M.: Polarisation of transverse sesmic waves. Geophys. J. Roy. Astron. Soc. **4**, 106–123, 1961

Dillinger, W.H., Harding, S.T., Hope, A.J.: Determining maximum likelihood body wave focal plane solutions. Geophys. J. Roy. Astron. Soc. **30**, 315–329, 1972

Engdahl, E.R., Kisslinger, C.: Seismological precursors to a magnitude 5 earthquake in the central Aleutian islands (supplement). J. Phys. Earth **25**, 243–250, 1977

Fuchs, K.: Das Reflektions- und Transmissionsvermögen eines geschichteten Mediums mit beliebiger Tiefenverteilung der elastischen Parameter und der Dichte für schrägen Einfall. Z. Geophys. **34**, 389–413, 1968

Fuchs, K., Müller, G.: Computation of synthetic seismograms with the reflectivity method and comparison with observations. Geophys. J. Roy. Astron. Soc. **23**, 417–433, 1971

Harjes, H.-P., Hinzen, K.-G., Cete, A.: Das Erdbeben bei Ibbenbüren am 13. Juli 1981. Geol. Jb. **E26**, 65–76, 1983

Hinzen, K.-G.: Vergleich von Herdflächenlösungen und Momententensoren. Ber. d. Inst. f. Geophysik d. Ruhr-Universität Bochum, Reihe A15, 1984

Kanasewich, E.R.: Time sequence analysis in geophysics. Edmonton: Univ. of Alberta Press 1975

Kisslinger, C.: Evaluation of S to P amplitude ratios for determini focal mechanisms from regional network observations. Bull. Seismol. Soc. Amer. **70**, 999–1014, 1980

Kisslinger, C., Bowman, J.R., Koch, K.: Procedures for computing focal mechanisms from local (*SV/P*)*z* data. Bull. Seismol. Soc. Amer. **71**, 1719–1729, 1981

Kind, R.: The reflectivity method for a buried source. J. Geophys. **44**, 373–383, 1978

Kind, R.: Extensions of the reflectivity method. J. Geophys. **45**, 373–383, 1979

Koning, L.P.G.: On the mechanism of deep focus earthquakes. Gerl. Beitr. Geophys. **58**, 159–197, 1942

Langston, C.A.: Single station fault plane solutions. Bull. Seismol. Soc. Amer. **72**, 729–744, 1982

Leydecker, G., Steinwachs, M., Seidl, D., Kind, R., Klassmann, J., Zerna, W.: Das Erdbeben vom 2. Juni 1977 in der norddeutschen Tiefebene bei Soltau. Geol. Jahrb. Reihe E 18, 3–18, 1980

Mooney, W.D., Prodehl, C.: Crustal structure of the Rheinish Massif and adjacent areas, a reinterpretation of existing seismic refraction data. J. Geophys. **44**, 573–601, 1978

Pearce, R.G.: Fault plane solutions using relative amplitudes of *P* and *pP*. Geophys. J. Roy. Astron. Soc. **50**, 381–394, 1977

Pearce, R.G.: Earthquake focal mechanisms from relative amplitudes of *P*, *pP* and *sP*: method and computer program. AWRE Report No 041/79, 1979a

Pearce, R.G.: Fault plane solutions using relative amplitudes of *P* and surface reflections: further studies. Geophys. J. Roy. Astron. Soc. **60**, 459–487, 1979b

Pearce, R.G.: Complex *P*-waveforms from a Gulf of Aden earthquake. Geophys. J. Roy. Astron. Soc. **64**, 187–200, 1981

Ritsema, A.R.: (I, Delta)- curves for bodily seismic waves of any focal depth. Lemb. Meteor. dan Geof. Djakarta, **54**, 1–25, 1958

Rummel, F., Baumgärtner, J.: Spannungsmessungen im östlichen Bereich der südwestdeutschen Scholle. Rep. Contr. No. RUB 7084408-82-3, Bochum, 1982

Rummel, F., Baumgärtner, J., Alheid, HJ.: Hydraulic fracturing stress measurements along the eastern boundary of the SW-German Block. In: Hydraulic fracturing stress measurements, proceedings of a workshop, Dec. 2–5, 1981, National Academy Press, Washington, 1983

Shapira, A., Båth, M.: Some mechanism determinations of short distance microearthquakes. Seis. Inst. Uppsala Rep., 1/78, 1–25, 1978

Stevens, A.E.: Earthquake mechanism determined by *S*-wave data. Bull. Seismol. Soc. Amer. **54**, 2034–2047, 1964

Udias, A.: A least squares method for earthquake mechanism determination using *S*-wave data. Bull. Seismol. Soc. Amer. **54**, 2037–2047, 1964

Received August 2, 1984; revised version December 6, 1984
Accepted December 7, 1984